Biogeochemistry
DOI 10.1007/s10533-012-9797-x

Interannual variation in seasonal drivers of soil respiration in a semi-arid Rocky Mountain meadow

Andrew B. Moyes · David R. Bowling

Received: 21 May 2012 / Accepted: 13 September 2012

Abstract Semi-arid ecosystems with annual moisture inputs dominated by snowmelt cover much of the western United States, and a better understanding of their seasonal drivers of soil respiration is needed to predict consequences of climatic change on soil CO_2 efflux. We assessed the relative importance of temperature, moisture, and plant phenology on soil respiration during seasonal shifts between cold, wet winters and hot, dry summers in a Rocky Mountain meadow over 3.5 separate growing seasons. We found a consistent, unique pattern of seasonal hysteresis in the annual relationship between soil respiration and temperature, likely representative for this ecosystem type, and driven by (1) continued increase in soil T after summer senescence of vegetation, and (2) reduced soil respiration during cold, wet periods at the beginning versus end of the growing season. The timing of meadow senescence varied between years with amount of cold season precipitation, but on average occurred 45 days before soil temperature peaked in late-summer. Autumn soil respiration was greatest when substantial autumn precipitation events occurred early. Surface CO_2 efflux was temporarily decoupled from respiratory production during winter 2006/2007, due to effects of winter surface snow and ice on mediating the diffusion of CO_2 from deep soil horizons to the atmosphere. Upon melt of a capping surface ice layer, release of soil-stored CO_2 was determined to be 65 g C, or ~10 % of the total growing season soil respiration for that year. The shift between soil respiration sources arising from moisture-limited spring plant growth and autumn decomposition indicates that annual mineralization of soil carbon will be less dependent on projected changes in temperature than on future variations in amount and timing of precipitation for this site and similar semi-arid ecosystems.

Keywords Carbon dioxide production · Soil gas profile · Respiration · Diffusion model · Phenology · Winter storage efflux

A. B. Moyes (✉) Moyes and Bowling at Utah
Department of Biology, University of Utah, 257 South, 1400 East, Salt Lake City, UT 84112, USA
e-mail: amoyes@ucmerced.edu

Only Moyes at Merced
A. B. Moyes · D. R. Bowling
School of Natural Sciences, University of California Merced, 5200 North Lake Road, Merced, CA 95343, USA

Introduction

Much of the semi-arid region in the western United States receives moisture primarily in the form of winter snow (Knowles et al. 2006). The most optimal growing conditions for pla[illegible]nd soil microorganisms in these ecosystems occur after snowmelt in spring, followed by a transition to summer drought limitation, and finally winter cold dormancy. During each of these phases, variations in climatic conditions, such as those

Journal : Medium 10533 | Dispatch : 21-9-2012 | Pages : 15
Article No. : 9797 | ☐ LE | ☐ TYPESET
MS Code : BIOG-D-12-00048 | ✔ CP | ✔ DISK

predicted for the region by climate simulations, are likely to affect photosynthetic and respiratory carbon fluxes in contrasting ways (Boisvenue and Running 2010; Richardson et al. 2010; Anderson-Teixeira et al. 2011). Changes to long-term soil carbon storage may represent a strong feedback between climate and ecosystem carbon balance, depending on cumulative impacts to litter production and decomposition (Schmidt et al. 2011). With climate predictions of western North America forecasting 2–6 °C warming by 2100 (IPCC 2007) and increased drought severity (Seager et al. 2007), an understanding of season-dependent interactions between abiotic conditions and plant and soil microbial activity is required to predict how soil respiration may affect soil carbon storage (Wardle 2004; Bardgett et al. 2005; Ryan and Law 2005; Moyes et al. 2010).

In snow-dominated ecosystems, the duration of snow cover and amount of water released on melting have a relatively strong impact on annual carbon inputs (Hu et al. 2010; Richardson et al. 2010). Snowpacks in the western U.S. are now melting earlier than in decades past (Cayan et al. 2001) and impacted by an increased proportion of winter precipitation is falling as rain (Gillies et al. 2012). These trends are largely attributed to human activity (Barnett et al. 2008) and expected to continue into the future (Boisvenue and Running 2010). Early snowmelt has been shown to lead to earlier onset of soil moisture stress and reduced productivity and soil CO_2 efflux (Sacks et al. 2007; Hu et al. 2010; Blankinship 2012), and may turn many western US ecosystems into net carbon sources (Anderson-Teixeira et al. 2011). Whether this happens will largely depend on the degree to which soil respiration is affected by changes in temperature, soil moisture, and available substrate over the year.

In seasonally drought stressed ecosystems ranging from cold deserts to subalpine forests, moisture limitation can inhibit soil respiration to varying degrees in summer, depending on amount of spring recharge of soil moisture and magnitude and timing of fall precipitation (Pacific 2009; Bowling et al. 2011). Although a few degrees of warming may exacerbate summer moisture stress, this may be more than compensated by increased soil respiration if moisture limitation is alleviated by autumn precipitation (Piao et al. 2008). Soil rewetting associated with drought-ending precipitation can immediately raise substrate availability to heterotrophic microorganisms and fuel a burst of microbial respiration (reviewed by Borken and Matzner 2009). However, rain pulses may stimulate widely varying amounts of soil respiration, depending on pulse size and timing, soil type, and the status of plants and soil microbes at the time of precipitation (Austin et al. 2004; Bowling et al. 2011). Given this uncertainty, it is imperative that we determine how changes in precipitation regime might affect total soil respiration from water-limited ecosystems.

Long-term (multi-year) data sets covering periods of interannual variability in seasonal weather are needed to understand the relative sensitivity of soil respiration to changing biotic and abiotic drivers (Fierer et al. 2005; Chou et al. 2008; Irvine et al. 2008). Unfortunately, relatively few long-term studies are available from snow-dominated, semi-arid ecosystems that typify much of western North America. In this study we sought to utilize interannual variability in precipitation to characterize the importance of drivers of soil respiration during seasonally contrasting periods of spring melt, summer drought, and autumn precipitation. We modeled soil CO_2 production from continuous automated soil CO_2 profile data collected in a Rocky Mountain meadow over 3.5 years, and compared production rates to temperature, moisture, and vegetation patterns. Our site was chosen to reflect general characteristics of snow-dominated, semi-arid ecosystems, and particularly those with herbaceous vegetation that senesces during summer moisture limitation. Our expectation was that predominant drivers of soil respiration would shift annually from vegetation to soil moisture to temperature, with the timing of these transitions dependent on the timing and amount of snowmelt and growing season precipitation.

Methods

Site description

Field measurements were made in a 4.3 ha meadow in Red Butte Canyon (111°47′46″W, 40°47′20″N, 1758 m elevation) above Salt Lake City, UT, USA. The meadow sits on a flat, open area of deep soil accumulated by downslope erosion of the steep, rocky canyon hillsides, which are vegetated primarily with

Journal : Medium 10533 | Dispatch : 21-9-2012 | Pages : 15
Article No. : 9797 | LE | TYPESET
MS Code : BIOG-D-12-00048 | CP | DISK

gambel oak (*Quercus gambelii*). A perennial stream flows along one side of the meadow, which is surrounded by riparian trees, of which boxelder (*Acer negundo*) and bigtooth maple (*Acer grandidentatum*) are most abundant. During the study, vegetation in the open meadow primarily comprised native and introduced herbaceous perennial and annual grasses and forbs, including mountain brome (*Bromus carinatus*), orchard grass (*Dactylus glomerata*), blue wildrye (*Elymus glaucus*), milfoil yarrow (*Achillea millefolium*), yellow sweetclover (*Melilotus officinalis*), dalmation toadflax (*Linaria dalmatica*), and hound's tongue (*Cynoglossum officinale*). Vegetation in the meadow began to grow soon after snowmelt, typically at around April 1, reached peak biomass around mid-June, and then senesced. The study site is beyond the reach of summer rain from the North American monsoon, and experiences cold, snowy winters and hot, dry summers (Ehleringer et al. 1992). Mean annual precipitation for the site is 500 mm, mostly falling in winter, and soils are loamy, deep, and well-drained (Ehleringer et al. 1992). Additional site details were given by Hultine et al. (2007).

Automated CO_2, moisture, and temperature profile measurements

Buried gas inlets and sensors were installed in the center of the meadow in June 2004. A pit with a surface area of ~ 0.5 m^2 was excavated to 50 cm depth. The surface soil horizons were placed to the side of the pit in large, intact pieces and were replaced after the pit was backfilled. Soil moisture sensors (CS615, Campbell Scientific, Logan UT, USA), thermocouples (Type T), and gas inlets were installed horizontally at 3, 10, 22, and 48 cm depths into intact soil through the wall of the pit, in non-overlapping positions. Each gas inlet consisted of a 25.5 cm length of 5 mm ID PTFE tubing (International Polymer Engineering, Tempe AZ, USA) within a protective length of 1.3 cm OD perforated polyethylene tubing. The PTFE tubing allowed diffusion of gases but prevented liquid water from being sampled (DeSutter et al. 2006), and was attached to sample tubing using 6.35 mm barb fittings with a cap at the distal end. The proximal end was attached to a 2-m length of 1.6 mm diameter stainless steel tubing. Fittings were held in place at the ends of the protective tubing with epoxy. Gas inlets were inserted through the pit wall by drilling pilot holes and tapping capped inlets into place, before removing the caps and attaching the sample tubing. Tubing and sensor wires were bundled and covered above ground until the measurement system was installed the following summer.

A soil gas measurement system was built following the design of Hirsch et al. (2002), but expanded to sample seven gas inlet lines on a regular schedule. Each gas inlet measurement cycle lasted 14 min, with 2 min for each of the seven inlet lines in the following order: calibration gas 1, calibration gas 2, +5 cm (just above the soil), −3, −10, −22, and −48 cm. A rotary valve (EMTCSD10MWM, Valco Instruments CO. Inc., Houston TX, USA) was used to cycle between inlet lines. Flow was driven by a pump (KNF Neuberger Inc., Trenton NJ, USA) or cylinder pressure (calibrations) and maintained at 50 standard ml min^{-1} by a mass flow controller (1179A, MKS Instruments, Andover MA, USA), downstream of an infrared gas analyzer (IRGA, LI-820, Li-Cor Biosciences, Lincoln NE, USA). Flow for each depth source was stopped after 75 s to allow gas in the IRGA measurement cell to return to ambient pressure, and data from the final 10 s were averaged. During measurements nitrogen gas flowed from a pressurized cylinder at 100 standard ml min^{-1} through a counterflow exchange tube (MD-050-12, Perma Pure LLC, Toms River NJ, USA) to dry sample gas prior to introduction to the IRGA. Solenoid valves were used to switch between calibration gases (WMO-traceable CO_2 in air standards). All sample flows were filtered to 2 μm (Alltech, Deerfield IL, USA).

The enclosure was connected to the buried inlet tubes and sensor wires on July 20, 2005, after which gas inlets and buried temperature and moisture sensors were measured every 1–4 h, depending on seasonally available sunlight used for power. Measurements continued, with some interruptions due to power loss and blockage of flow in winter (probably related to freezing water in inlet tubes), until late November of 2008. An ultrasonic snow depth sensor (Judd Communications, Salt Lake City UT, USA) was installed in the meadow near the soil profile measurements during each winter.

Laboratory measurements of soil tortuosity

To parameterize a diffusion model from soil profile data, soil tortuosity factors were calculated from intact soil cores in the laboratory using controlled diffusion

Journal : Medium 10533 | Dispatch : 21-9-2012 | Pages : 15
Article No. : 9797 | LE | TYPESET
MS Code : BIOG-D-12-00048 | CP | DISK

experiments following Jassal et al. (2005). To check for variability in tortuosity with depth and horizontal position, soil cores were collected from two locations at 10 cm depth intervals to 50 cm in the meadow using 10-cm diameter PVC tubing. After collection, soil was held in place in the core with a metal screen. Soil cores were taken to the laboratory and wetted to field capacity. A series of measurements of induced CO_2 fluxes was made over the maximum range of water content for each core (field capacity to oven dried) to calculate a fitted tortuosity versus air-filled porosity function. Calculations accounted for CO_2 production within the core. Soil moisture within the cores was allowed to equilibrate between incremental changes in wetness by sealing each core inside an air-tight bag for at least 1 week. Total porosity of soil cores was calculated from dry bulk density, assuming a solid particle density of 2.65 g cm^{-3}. Air-filled porosity was obtained by subtracting the volume of water from the total pore space.

Model calculation of fluxes and production

Molar density of CO_2 (μmol m^{-3}) in the meadow soil profile was calculated from CO_2 mol fraction, air pressure, and temperature profile data. A second-order polynomial function was fit to each set of CO_2 molar density data versus depth for each profile measurement cycle. The first derivative of this function was calculated for the surface ($z = 0$) and each measurement depth, and these values were used as CO_2 gradients (dC/dz) in flux calculations following Fick's first law of diffusion:

$$F = -D\frac{dC}{dz} \quad (1)$$

where F is the flux density of CO_2 across a horizontal plane at each measurement depth (μmol m^{-2} s^{-1}), and D is the diffusion coefficient of CO_2 in soil pore air. Diffusion coefficients were calculated for each measurement depth and time following:

$$D = D_o \times \xi \quad (2)$$

with D_o being the diffusion coefficient of CO_2 in air, given by:

$$D_o = D_{ao}\left(\frac{T}{293.15}\right)^{1.75}\left(\frac{101.3}{P}\right) \quad (3)$$

where P is 82 kPa (local atmospheric pressure for the site) and T is the soil temperature at the relevant depth and time (Massman 1998). D_{ao} is 15.7 mm^2 s^{-1}, the reference value for CO_2 in air at 293.15 K and 101.3 kPa. ξ is a dimensionless tortuosity factor, which was calculated using the power function fit to soil core data from the laboratory diffusion experiment. This relationship was not different between soil depths or the two meadow positions sampled (shown below), so the following function derived from the entire data set was used:

$$\xi = 0.95\varepsilon^{1.93} \quad (4)$$

where ε is the air-filled porosity (m^3 m^{-3}) calculated for each soil measurement depth and time from total porosity and volumetric water content. Rates of production of CO_2 (μmol m^{-3} s^{-1}) within depth intervals between measurements were calculated as the difference in CO_2 flux densities across the upper and lower depth limits multiplied by the difference in depth (de Jong and Schappert 1972).

Continuous soil chamber measurements

An open chamber system was built and installed at the meadow site between July 10 and November 9, 2008 to provide CO_2 surface flux density measurements to constrain the diffusion model results. The chamber was designed following Rayment and Jarvis (1997) and was inserted several cm into bare soil within 2 m of the soil profile measurements. The system was controlled by a datalogger (CR5000, Campbell Scientific, Logan UT, USA), programmed to sample every fourth day to conserve solar power. On sampling days a pump (KNF Neuberger, Trenton NJ, USA) was turned on at midnight and for 24 h continuously pulled air through the chamber at 1.5 standard l m^{-1} and from the inlet flow of the chamber at 500 standard ml min^{-1}. A second pump was used to pull subsample flows at 150 standard ml min^{-1} individually from the chamber inlet and outlet flows through an IRGA (LI-800, Lic-Cor Biosciences, Lincoln NE, USA). The chamber flux was measured every 2 h beginning at 1 a.m., and each measurement cycle began with measurements of CO_2-free air and a calibration gas. Switching between all gas sources was controlled using solenoid valves (Clippard Instrument Laboratory, Inc., Cincinnati OH, USA), and all flows were controlled using variable area flow meters (Gilmont Instruments, Barrington IL, USA). Flows were stopped prior to all CO_2 measurements to allow the IRGA measurement cell to stabilize at atmospheric

Journal : Medium 10533 | Dispatch : 21-9-2012 | Pages : 15
Article No. : 9797 | LE | TYPESET
MS Code : BIOG-D-12-00048 | CP | DISK

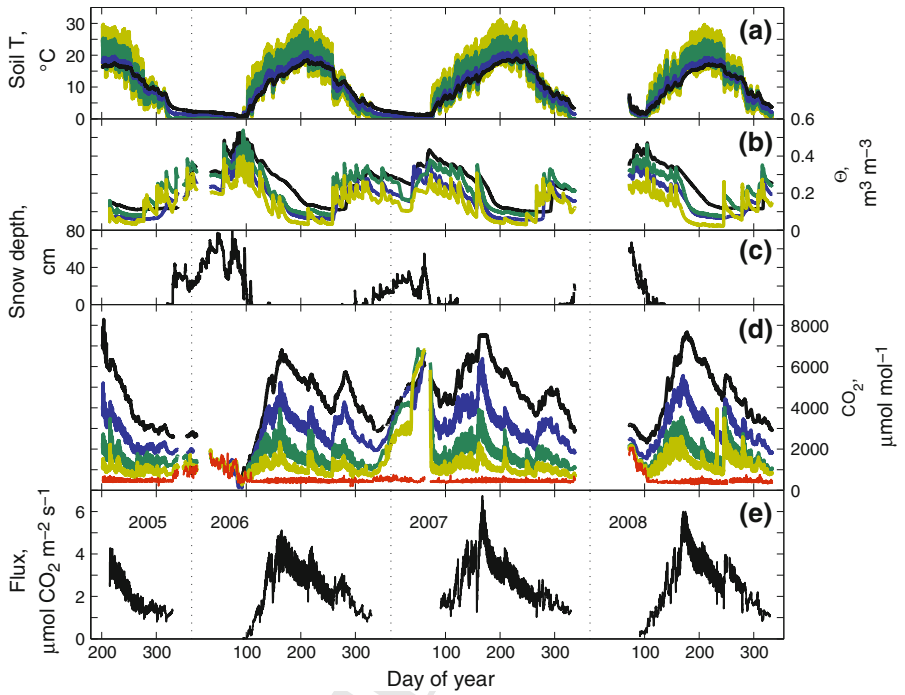

Fig. 1 Soil temperature (**a**), volumetric water content (θ, **b**), snow depth (**c**), belowground CO_2 (**d**), and modeled surface CO_2 flux (**e**) over the entire study period. In **a**–**d**, data from within the soil are shown as *colored lines shaded* from *lightest* to *darkest* for depths of 3, 10, 22, and 48 cm. Mole fraction of CO_2 from 5 cm above the soil surface is shown in (**d**) as a *red line*. *Vertical dotted lines* indicate the beginning of each calendar year

pressure. The dilution effect of water vapor in inlet and outlet flows was corrected by placing a humidity sensor (HMP45A, Vaisala, Woburn MA, USA) in-line, upstream of the IRGA. Surface CO_2 flux rates were calculated using:

$$Flux = \frac{(C_o - C_i)Flow}{A} \quad (5)$$

where C_o and C_i are the mole fractions (µmol mol^{-1}) of CO_2 in air in the inlet and outlet flows from the chamber, "Flow" is moles of air passing through the chamber per second (mol s^{-1}), and A is the soil surface area enclosed by the chamber (m^2). The chamber remained in a single position until rain events, after which it was moved and inserted into the soil at another nearby bare soil location, with no further measurements occurring on the same day the chamber was moved.

Results

Profile measurements

Soil temperature varied between 0 and 30 °C annually, with maximum seasonal and diel temperature variability near the soil surface (Fig. 1a). Temperature in the soil under snow cover (Fig. 1c) slowly declined over the winter and remained above freezing. Soil moisture was consistently highest in the cold months of the year, and decreased during spring/summer following snow melt (Fig. 1b, c). Summer reduction of soil moisture was greatest near the soil surface. The timing and magnitude of late summer and fall precipitation events varied from year to year.

Carbon dioxide typically increased with depth and varied seasonally (Fig. 1d), with highest mole fractions measured in mid-June, about 1.5 months before soil temperature reached the seasonal maximum (Fig. 1a). Additional transient CO_2 peaks occurred in the soil following summer and fall rain events. Profiles of CO_2 under snow cover were markedly different between winters. In winter 2005/2006, soil CO_2 mol fraction decreased during spring melt until the entire measured profile nearly matched the atmosphere (Fig. 1c, d). In winter 2006/2007, decoupling of soil CO_2 and the atmosphere was apparent as CO_2 mol fraction increased in the shallow soil and equilibrated with CO_2 stored in deeper layers.

Diffusion model results

Throughout the following we refer to "surface CO_2 efflux" as the flux density of CO_2 (µmoles CO_2 m^{-2} s^{-1}) calculated for the soil surface from

Journal : Medium 10533 | Dispatch : 21-9-2012 | Pages : 15
Article No. : 9797 | LE | TYPESET
MS Code : BIOG-D-12-00048 | CP | DISK

the diffusion model or continuous chamber data, "CO_2 production" as the rate of respiratory production of CO_2 calculated with the diffusion model for specific zones within the soil profile (μmoles CO_2 m^{-3} s^{-1}), and "soil respiration" as the interpreted true instantaneous rate of soil CO_2 production by the entire soil profile. Surface CO_2 efflux would only reflect total CO_2 production and soil respiration under conditions of steady state.

Modeled fluxes incorporated the composite measured tortuosity relationship with air-filled porosity from all soil cores (Eq. 4). This fitted function was similar to relationships published by Millington (1959) and Jassal et al. (2005) (Fig. 2a). Soil respiration patterns within the study period were not strongly affected by choosing one of these other tortuosity functions (data not shown). Hourly variability in modeled fluxes (Fig. 1e) reflected rapid changes in soil CO_2, T, and θ, via effects on soil CO_2 production and diffusivity. However, the amplitude of diel surface CO_2 flux variability in chamber observations was much larger than was produced by the model during summer/fall 2008, when both methods were applied simultaneously (Fig. 2b, c). Surface efflux variability measured with the chamber was taken as a more direct, and thus reliable measure, and for this reason daily means of modeled flux and production results were used in subsequent analyses.

Seasonal drivers of soil respiration

During the snow-free growing season (approximated as days 100–330 across years for comparison) surface fluxes increased steeply during spring, and decreased more gradually over summer and fall, with additional, smaller peaks appearing after rain events (Fig. 3). Daily CO_2 production was generally larger over the 0–22 cm depth interval than from 22 to 48 cm (Fig. 3c, d). The sum of these sources accounted for nearly all the surface flux (representing total soil production at steady state), suggesting that relatively little CO_2 production occurred below 48 cm. Daily

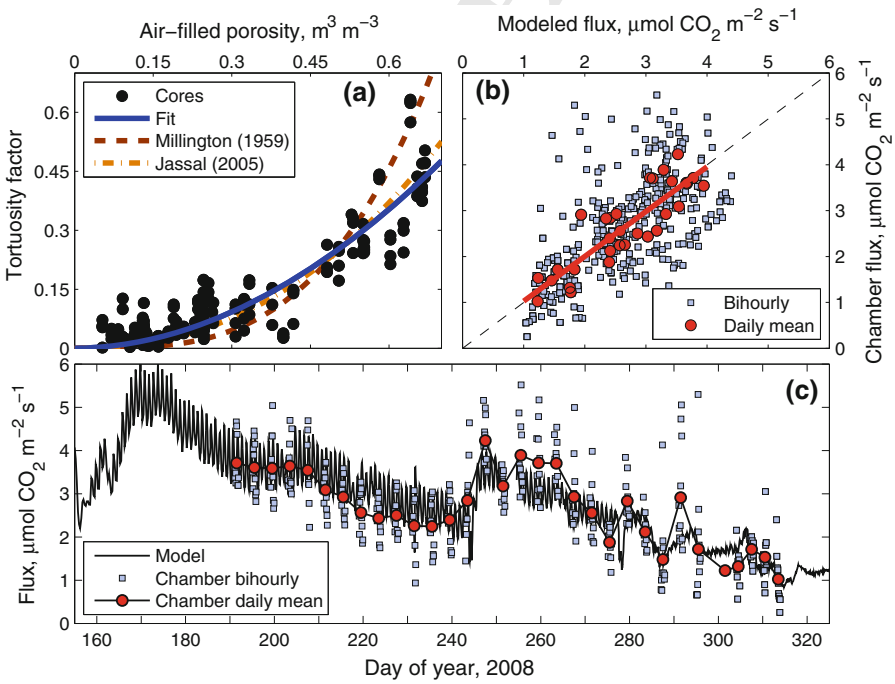

Fig. 2 **a** Calculated tortuosity factors (dimensionless) from laboratory measurements of soil cores evaluated over a range of air-filled porosities, with a fitted power function (Eq. 4) and relationships published by Millington (1959) and Jassal et al. (2005) presented for comparison. **b** Comparison of surface fluxes calculated with the model and measured with an *open* soil chamber placed on *top* of the soil near the buried soil gas inlets. Model results and chamber data are shown for each of the bihourly chamber measurement periods, in addition to daily mean fluxes for both methods. The *1:1 line* is shown for comparison. The *red line* is fit to daily mean data, and is $y = 0.98x + 0.05$, $p < 0.001$, $r^2 = 0.75$. **c** Time series of modeled surface fluxes and bihourly and daily mean *open* soil chamber measurements during summer and fall 2008

Journal : Medium 10533 | Dispatch : 21-9-2012 | Pages : 15
Article No. : 9797 | LE | TYPESET
MS Code : BIOG-D-12-00048 | CP | DISK

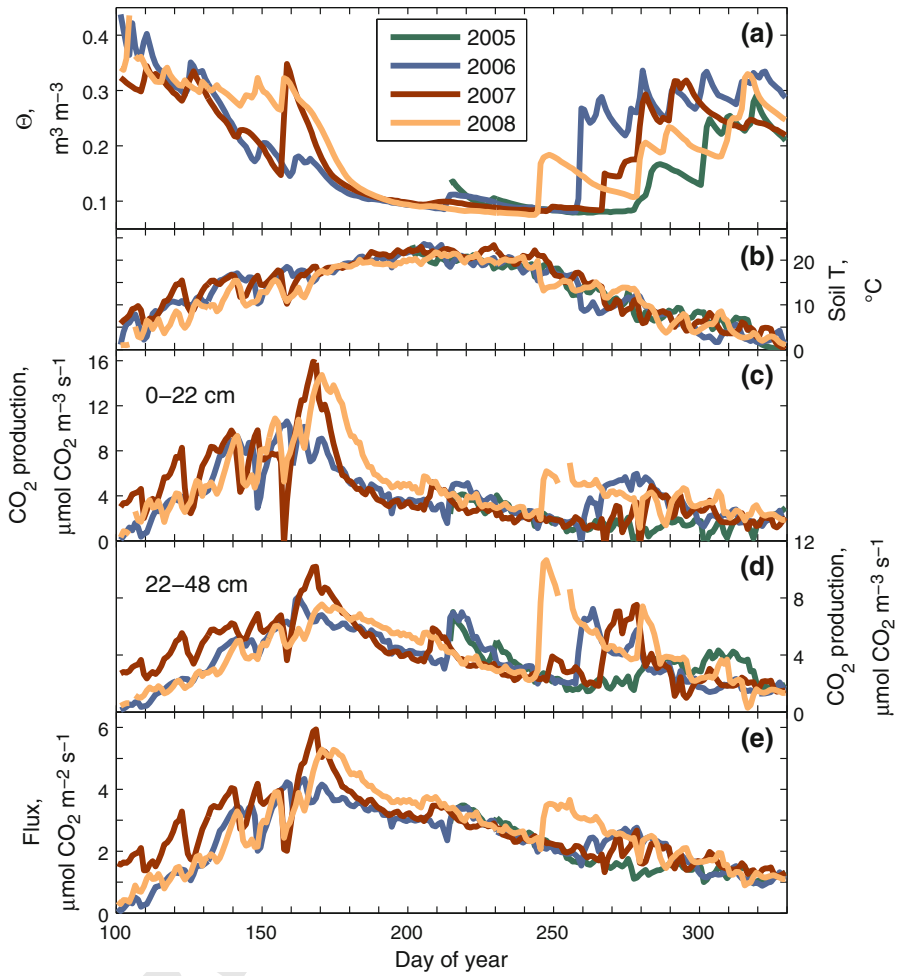

Fig. 3 Daily means of volumetric water content at 10 cm (θ, **a**), soil temperature at 10 cm (**b**), calculated CO_2 production rate for soil within the 0–22 (**c**) and 22–48 cm (**d**) ranges of soil depth, and modeled CO_2 surface flux (**e**) for each growing season during the study

average soil respiration fluxes peaked sharply in mid-June for all years at 4–6 µmol m^{-2} s^{-1} (~4–6 g C m^{-2} day^{-1}, Fig. 3e). Model results indicated that late summer CO_2 production spiked at both depth intervals after rains, though often these rain events did not penetrate deep into the soil (Fig. 3b). Soil moisture at 10 cm reached similar seasonal summer minima during all years studied. Modeled shallow soil CO_2 production and surface CO_2 flux peaks were synchronized with the timing of drawdown of spring soil moisture, rather than the seasonal pattern of soil temperature (Fig. 3). Cumulative soil CO_2–C efflux from the model for each entire snow-free period was 559, 631, and 622 g C m^{-2} $year^{-1}$ for 2006, 2007, and 2008, respectively.

Relationships between soil temperature and soil respiration followed three consistent seasonal trajectories within each year (Fig. 4). The transitions between these phases were evident in the rates of change (first derivatives with respect to time) of temperature, surface CO_2 efflux, and soil moisture calculated for sets of five consecutive days, averaged across all years of this study (Fig. 5). In the first period (P.1, days 100–169), defined as the time between snowmelt and peak biomass and maximum soil respiration (which co-occurred), soil respiration increased steeply with soil temperature. In the second period (P.2, days 170–213), defined as the period from peak biomass (and initiation of senescence) to maximum soil temperature, soil respiration decreased while soil temperature continued to increase. In period 3 (P.3, days 214–330), representing the time from maximum soil temperature to onset of winter precipitation, soil respiration and soil temperature decreased together. While large variations in temperature, moisture, and respiration fluxes associated with synoptic weather events during periods 1 and 3 were apparent after

Journal : Medium 10533 | Dispatch : 21-9-2012 | Pages : 15
Article No. : 9797 | LE | TYPESET
MS Code : BIOG-D-12-00048 | CP | DISK

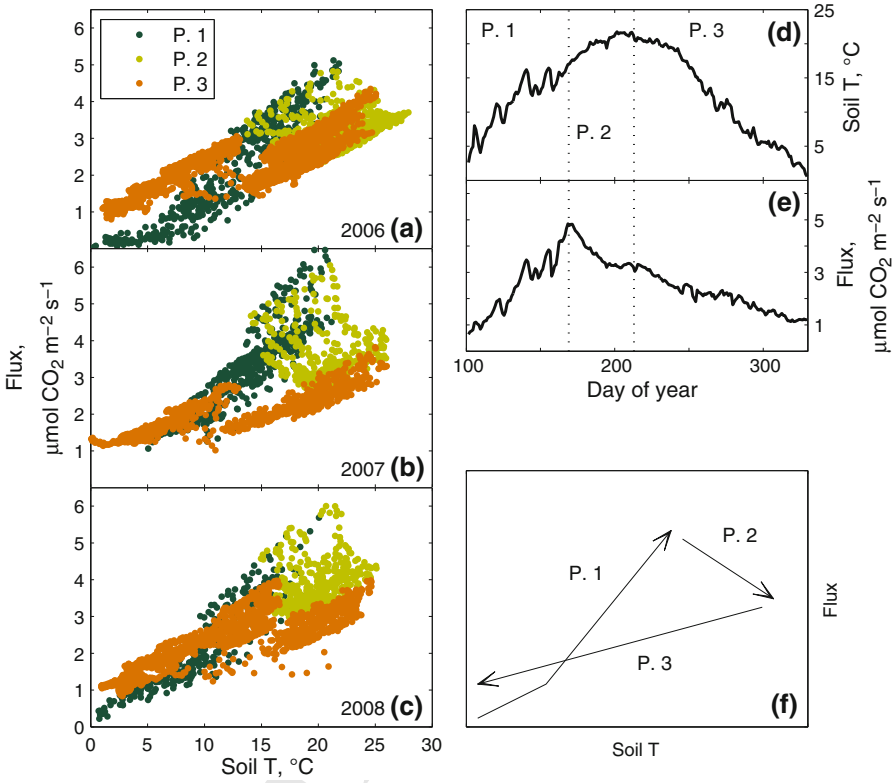

Fig. 4 **a–c** Modeled surface CO_2 flux versus soil temperature at 10 cm for each of the three complete growing seasons of the study. Each season was divided into three periods (P.1–3), with the first division (day 169) identified as the day of maximum surface CO_2 efflux from averaged model results for all 3 years (**e**), and the second division (day 213) identified as the average day of seasonal maximum soil temperature at 10 cm (**d**). **f** A schematic representation of the relationship between CO_2 flux and soil temperature over the seasonal course of the three periods. Respiration and temperature patterns during winter periods (not included in this study) would be needed to connect the end of P.3 to the beginning of P.1

averaging all years consistently warm and dry conditions during period 2 corresponded with a relatively smooth increase in the average rate of change in soil moisture towards zero.

In addition to soil moisture and temperature effects during the snow-free period, winter freezing of water at and above the soil surface was determined to impact modeled surface fluxes into the 2007 growing season, although soil temperature at 0.5 cm did not go below 0 °C (Fig. 1a). In contrast to the 2005/2006 winter, CO_2 in the snow (+5 cm above soil surface) during 2006/2007 was decoupled from the soil profile and reflected mole fractions similar to the convectively-mixed air above the snow (Fig. 1d). Snow accumulated slowly in this winter, with frequent melting and some precipitation arriving as rain. Wet soil at the surface and cold temperature appeared to inhibit CO_2 diffusion from the soil to the atmosphere, as CO_2 mol fractions at depth increased during this time of low snow cover (Fig. 1d). Later in this winter an ice layer developed several centimeters thick, after a melt period was followed by a storm (Fig. 1b–d). At this time, CO_2 mol fraction at the shallow measurement depths rose suddenly and very sharply, and equilibrated with values at the deepest depths (Fig. 1d). Just before the ice and snow melted (March 3), rather than a progressive decrease in soil CO_2 profile via diffusion to the atmosphere (Fig. 6a), an inverted CO_2 gradient (decreasing mole fraction with increasing depth) was apparent in the measured profile (Fig. 6b). This indicated that shallow soil winter CO_2 production was occurring and producing a net downward CO_2 flux, and enhancing storage of CO_2 in soil pores under the ice. Within a month after the ice melted and diffusion to the atmosphere was again restored (April 4), a more typical profile of increasing CO_2 with depth was observed. Model results indicated that loss of soil storage of CO_2 led to an initial increase in surface flux of 1–2 µmol m^{-2} s^{-1}, or about 10 times the average surface efflux following snowmelt in the other measured years (Fig. 7). This relative increase dropped rapidly over the next few weeks, but growing season surface fluxes did not consistently match the average of other years until after about 40 days after the surface ice diminished and the diffusive storage efflux peaked. If the efflux of winter-stored soil CO_2 was entirely responsible for surface flux differences between 2007 and other years during the period following melt (Fig. 7), total winter storage loss (integration of Fig. 7a)

Journal : Medium 10533 | Dispatch : 21-9-2012 | Pages : 15
Article No. : 9797 | LE | TYPESET
MS Code : BIOG-D-12-00048 | CP | DISK

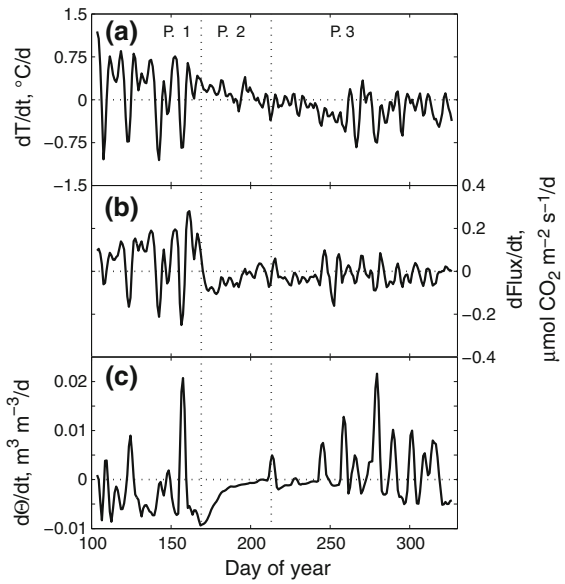

Fig. 5 Rates of change in soil T at 10 cm (**a**), surface CO_2 flux (**b**), and volumetric water content at 10 cm (θ, **c**) for successive 5-day windows of daily-averages from all years. Values above zero indicate increasing and values below zero indicate decreasing. Transitions between periods 1–3 can be seen as the points where dFlux/dt (P.1/P.2) and dT/dt (P.2/P.3) change sign (cross zero). Rates show sporadic changes during periods 1 and 3, when inter-annual variability in large weather events was high, but are more consistent during P.2. In P.2, soil temperature continued to increase (**a** *line* remains above zero), fluxes began to decrease (**b** *line* crosses zero and stays negative), and soil moisture depletion sharply decreased and then ended (**c** *line* increases asymptotically to zero)

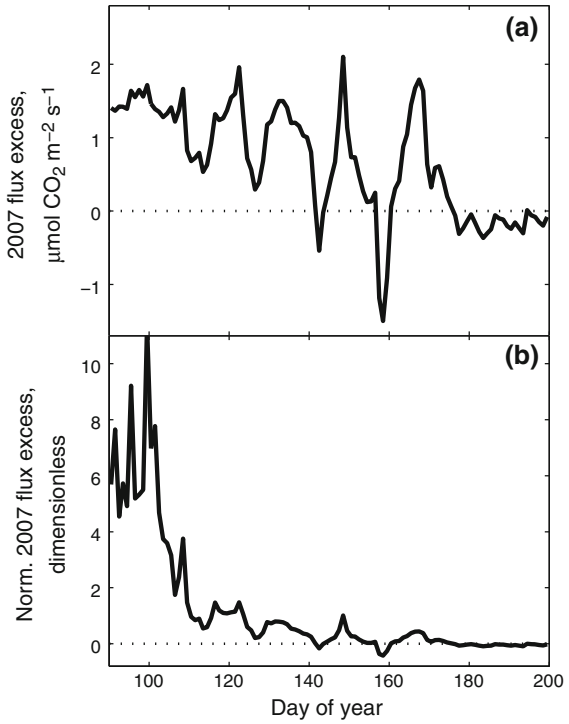

Fig. 7 Difference between modeled surface CO_2 flux following snowmelt in 2007 and the average of the other years studied, expressed as absolute (**a**) and normalized (difference/mean, **b**) excess (labeled as "excess" flux to reflect its possible source from stored soil CO_2 rather than concurrent respiratory production)

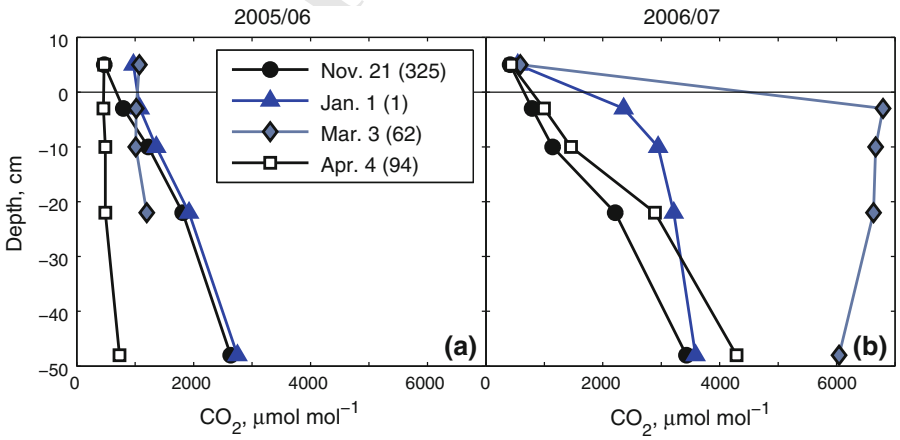

Fig. 6 Vertical profiles of CO_2 within the soil measured at specific dates during the 2005/2006 (**a**) and 2006/2007 (**b**) winters, shown to highlight the inter-annual differences. Dates and day of year are indicated in the legend. An inverted CO_2 gradient (CO_2 decreasing with depth) is seen in March 2007, indicating a downward flux increasing soil CO_2 storage

Journal : Medium 10533 | Dispatch : 21-9-2012 | Pages : 15
Article No. : 9797 | LE | TYPESET
MS Code : BIOG-D-12-00048 | CP | DISK

was 64.5 g C, or ~10 % of total growing season soil respiration. Removing this storage efflux enhancement would reduce the 2007 growing season soil respiration total to 567 g C.

Discussion

We utilized interannual variability in precipitation to evaluate seasonal drivers of soil respiration in a semi-arid, snow-dominated mixed grassland, providing a relatively complete perspective on soil respiration sensitivity to environment in this widespread ecosystem type. We identified three time periods between snowmelt and winter with contrasting limitations to soil respiration. Period 1 was from snowmelt to peak biomass (~day 169), during which soil respiration was linked to plant growth and activity, with a primary importance of winter and spring precipitation. Period 2, from peak biomass until peak soil T, was characterized by consistently dry soil, senescent vegetation, and an absence of precipitation. Period 3, after temperature had begun to cool, was associated with variable summer/fall precipitation events, to which soil respiration was highly responsive. In each of these periods, soil respiration rates were sensitive to contrasting climate conditions, leading to varied implications for the net effect of predicted climate changes on annual soil respiration. We expect that these seasonal conditions may exist in other snow-dominated, semi-arid ecosystems where summer precipitation is minimal and autumn precipitation is variable.

Period 1

Following snowmelt, meadow vegetation was emerging from seed and perennating buds, and thus aboveground biomass and presumably autotrophic soil respiration were minimal. Cold periods immediately after snowmelt showed the lowest soil respiration rates in most years, but efflux rates increased steeply to an annual maximum as soils warmed and vegetation grew to peak biomass (Figs. 4, 5). This steep increase was likely fueled by metabolism of recent photosynthate transported belowground during growth of meadow vegetation (Vargas 2011).

Peak biomass coincided with the greatest rates of soil CO_2 production and the depletion of winter and spring soil moisture, with wetter years (e.g. 2008) producing later and larger spring peaks in CO_2 production and fluxes (Fig. 3). At the point of peak biomass, when the CO_2 surface flux peaked and began to decrease sharply, the rate of soil moisture depletion at 10 cm reached a maximum (most negative $d\theta/dt$ in Fig. 5c). Then soil moisture loss rapidly slowed down, coinciding with senescence of vegetation, and likely attributable to a sharp decrease in transpiration flux of water out of the soil. The observation that soil respiration dropped sharply during senescence while soil moisture remained relatively constant (Fig. 5) implies that soil respiration during Period 1 had been strongly associated with plant activity. The similarity of minimum soil moisture at 10 cm during summers of all years (~0.08 m^3 m^{-3}, Fig. 3a) may indicate a minimum water potential threshold for water uptake at this site (Sperry 2000).

Period 2

The summer period between peak biomass and maximum soil temperature was the most consistent across years in terms of interannual variability, being consistently warm and absent precipitation, with declining soil respiration (Figs. 3, 5). Soil respiration was likely increasingly substrate-limited as photosynthetic assimilation decreased and plant carbon allocation may have been directed towards reproduction for annual plants. Additionally, existing dissolved soil organic carbon would have become progressively less available to microorganisms as soils became very dry (Skopp et al. 1990; Howard and Howard 1993; Davidson and Janssens 2006). The resulting midsummer depression of soil respiration was similar to that observed in Mediterranean zones where vegetation senesces or becomes inactive during similarly hot and dry summers (Tang and Baldocchi 2005; Chou et al. 2008; de Dato et al. 2010).

Period 3

Small midsummer rains occurred in all years around day 220 and wet surface soils briefly before being lost to evapotranspiration (Fig. 1b). While these small events led to increased soil CO_2 (Fig. 1d), the corresponding decrease in modeled diffusion coefficient due to wetting almost entirely offset the increase in CO_2 gradients, leading to a minimal increase in the calculated surface flux (Fig. 3). These results are

Journal : Medium 10533 | Dispatch : 21-9-2012 | Pages : 15
Article No. : 9797 | LE | TYPESET
MS Code : BIOG-D-12-00048 | CP | DISK

consistent with findings of Olsen and Van Miegroet (2009), who found short-lived (<1 week) increases in soil respiration following July and August irrigations of 2.5 cm water to northern Utah rangelands. Their results and ours suggest a more complete rewetting of the soil profile is necessary to achieve a substantial and sustained respiratory response (Fig. 3).

Continued cooling temperature within Period 3 was associated with larger, drought-ending precipitation events. Soil respiration responses to large summer/fall rain events varied among years with the timing and amount of precipitation. Comparisons of rain event responses in Fig. 3 suggest that earlier and larger summer/fall rains were associated with larger increases in respiratory production and surface CO_2 efflux than later and smaller rains, as reported for other ecosystems (Chou et al. 2008; Munson et al. 2010). Relatively early fall rains in 2008 produced a large and sustained increase in soil respiration compared to other years, in which larger rain events occurred later in the season (Figs. 3, 4). Decreasing respiratory responses to drought-ending precipitation with time in season could possibly explained by declining soil temperature (Figs. 3, 4). Additionally, more substrate may have been available for decomposition at the time of rainfall in 2008, given the longer period of spring soil moisture availability (Fig. 3), and thus potentially greater plant growth and litter production. Although a small amount of plant growth was observed after fall rains, the large increase in soil respiration following summer and fall rains after soil temperatures peaked (within Period 3) was probably mostly due to stimulated heterotrophic respiration. Mechanisms for rain pulse-induced peaks in heterotrophic soil respiration include decomposition of dissolved labile soil organic carbon (Saetre and Stark 2005; Borken and Matzner 2009; Chen et al. 2009) and mineralization of intracellular solutes during microbial adjustments to the rapid change in osmotic conditions (Fierer and Schimel 2003). Further analysis, such as soil rewetting experiments (Miller et al. 2005; Kim et al. 2012), would be needed to determine causes of the variable responses of soil respiration to rain we observed.

Winter

At the end of Period 3, just before snowfall, soil respiration rates were higher for a given temperature than rates associated with the same temperature during Period 1 (Fig. 4), although both of these seasonal phases were associated with similarly high soil moisture (Fig. 3). Greater respiration in fall than spring may have been due to the greater amount of soil carbon available for decomposition in fall due to litter input from senescent plant tissues above- and below-ground. Lower respiration rates in spring with adequate moisture and similar temperature imply that at the time of green up of the meadow in spring, heterotrophic soil respiration was substrate-limited. One apparent exception to this pattern was spring 2007, when early spring respiration rates for a given temperature were as high as rates during the fall (Fig. 4). However, the 2007 growing season followed the unique winter within this study when CO_2 accumulated in soil pores beneath an ice layer (Figs. 1, 6). As soils at the site were extremely deep, with unsaturated, porous soil extending for several meters (data not shown), the cause of the uniquely high early season fluxes in 2007 was probably efflux of CO_2 stored in the soil from winter and the previous growing season (2006). This conclusion was supported by the decreasing offset between CO_2 surface fluxes (and production attributed to both depth intervals) in 2007 and those of other years over the first few weeks after snow melt (Figs. 6, 7). The long duration of excess surface CO_2 efflux (Fig. 7) may have been due to low diffusivity of very wet soils (e.g. $\theta > 0.3$, $\varepsilon < 0.15$) following snowmelt (Fig. 2).

Implications for annual soil carbon balance

Cumulative soil respiration during the growing season (63 % of the year from day 100 to 330) ranged from 559 to 622 g C m^{-2} $year^{-1}$, which corresponds well with published estimates for temperate grasslands (Raich 1992; Bond-Lamberty and Thomson 2010). Heterotrophic soil respiration at this site may be enhanced by carbon subsidies (litterfall) from nearby deciduous trees. Lacking detailed measurements of physical attributes of the snowpack, we were unable to model respiration fluxes under snow, which likely contributed a substantial amount to the annual soil CO_2 flux (Brooks et al. 2005; Liptzin et al. 2009). Evidence of under-snow CO_2 production included an inverted CO_2 gradient under capping ice at the surface (Fig. 6) and the difference in fall and spring relationships between surface CO_2 efflux and soil T (Fig. 5). It appeared that fall and winter decomposition had

Journal : Medium 10533 | Dispatch : 21-9-2012 | Pages : 15
Article No. : 9797 | LE | TYPESET
MS Code : BIOG-D-12-00048 | CP | DISK

diminished the carbon inputs from each growing season by the time of the following spring, so that heterotrophic respiration was substrate limited at the time of snowmelt. This interpretation is consistent with glucose addition experiments in winter showing microbial respiration under snow to be carbon limited in the Rocky Mountains (Brooks et al. 2005). A visibly-bleached and compressed litter layer was present immediately after each snowmelt, but then disintegrated and almost entirely disappeared by the time of emergence and growth of vegetation. No permanent litter layer or thatch remained on the soil surface of the meadow into summer. Readily-decomposable (e.g. herbaceous) litter may undergo 50–80 % of annual decomposition under snow in mountain sites (Coxson and Parkinson 1987; Baptist et al. 2010), whereas in nearby sites with more recalcitrant litter, winter decomposition may account for much less (e.g. 10–16 % in a coniferous forest (Kueppers and Harte 2005)). While a high potential for winter decomposition may compensate for interannual variability in litter production at this site, further study is necessary to determine how slow-turnover soil carbon pools are impacted during periods of spring plant growth and autumn/winter decomposition.

Model performance

Our modeling approach was relatively simple and omitted factors such as storage in liquid and gas phases (Simunek and Saurez 1993; Gamnitzer et al. 2011), advection (Camarda et al. 2007; Flechard et al. 2007), and transport and heat conduction lags (Maseyk et al. 2009; Phillips et al. 2011). Dissolution of CO_2 in the highly calcareous soil, while not represented in our model, may explain how an increased CO_2 flux may have been sustained for several weeks into 2007 from CO_2 stored under capping ice (Fig. 8) (Gamnitzer et al. 2011). The limited daily flux variability produced by the model in comparison with flux variability measured with a soil chamber (Fig. 2) may reflect a violation of the steady state assumptions implicit in our model approach. Closer correspondence over hourly timescales was reported when similar model and chamber approaches were compared in a forest in Vancouver, Canada (Jassal et al. 2005). It may be that greater surface temperature variability at our more arid site led to greater flux variability than our steady state model could reproduce. The disparity between performance of their model and ours is unlikely a result of differences in soil structure, given the similarity of our soil tortuosity relationships to soil moisture (Fig. 2a). As reported by Riveros-Iregui (2008), model-chamber agreement was reduced when water content was very high or changed abruptly due to rain events. In spite of these limitations, daily average flux results from the model captured soil respiration variability in continuous chamber measurements over the dynamic late summer of 2008 (Fig. 2), reflecting adequate model performance for the purposes of this study.

Summary

Semi-arid, snow-dominated ecosystems of the intermountain western U.S oscillate annually between cold/wet and warm/dry conditions. This generates a strong seasonality and path-dependence (importance of antecedent conditions) in the drivers of soil respiration, and complicates predictions about responses of soil respiration to climate change. We found a recurrent seasonal hysteresis in the relationship between soil respiration and soil temperature that resulted from shifting relationships between soil temperature, moisture, and substrate supply to roots and soil heterotrophs. While we have not seen a similar pattern published to date, we expect it may occur in other snow-dominated ecosystems with minimal summer precipitation. Soil respiration in spring was tightly coupled to plant activity, reaching an annual maximum at peak aboveground biomass, when winter and spring soil moisture had been depleted to $\sim 0.1\ m^3\ m^{-3}$ at 10 cm depth. Then, senescence and continued soil drying led to decreased soil respiration despite continued increases in temperature. Fall precipitation stimulated widely varying amounts of soil respiration, with indications that earlier and larger fall rain events may stimulate greater soil CO_2 production. High fall rates of soil respiration persisted until snowfall, with late fall soil respiration greater than found in early spring for a given temperature. We also observed a noteworthy period of winter soil CO_2 storage accumulation beneath surface ice in 2007, which enhanced modeled efflux for several weeks after melt. A consistent theme in all of these observations is a dependence of soil respiration on both current and antecedent environmental and biotic conditions. Finally, we conclude that the amount and timing of winter and spring precipitation (promoting

Journal : Medium 10533 | Dispatch : 21-9-2012 | Pages : 15
Article No. : 9797 | LE | TYPESET
MS Code : BIOG-D-12-00048 | CP | DISK

vegetation growth) and summer and autumn precipitation (promoting decomposition) will determine how soil respiration responds to climate change in this and similar sites.

Acknowledgments A.B. Moyes is grateful for funding during this project from the A. Herbert and Marian W. Gold scholarship. Greg Winston provided helpful discussions about the design of the soil CO_2 sampling system. Sarah Gaines was tremendously helpful with the soil core diffusion measurements in the lab. Soil profile data will be made available for collaborative use upon request—contact the senior author. This study was funded by the University of Utah.

References

Anderson-Teixeira KJ, Delong JP, Fox AM, Brese DA, Litvak ME (2011) Differential responses of production and respiration to temperature and moisture drive the carbon balance across a climatic gradient in New Mexico. Glob Chang Biol 17:410–424

Austin AT, Yahdjian L, Stark JM, Belnap J, Porporato A, Norton U, Ravetta DA, Schaeffer SM (2004) Water pulses and biogeochemical cycles in arid and semiarid ecosystems. Oecologia 141:221–235

Baptist F, Yoccoz N, Choler P (2010) Direct and indirect control by snow cover over decomposition in alpine tundra along a snowmelt gradient. Plant Soil 328:397–410

Bardgett RD, Bowman WD, Kaufmann R, Schmidt SK (2005) A temporal approach to linking aboveground and belowground ecology. Trends Ecol Evol 20:634–641

Barnett TP, Pierce DW, Hidalgo HG, Bonfils C, Santer BD, Das T, Bala G, Wood AW, Nozawa T, Mirin AA, Cayan DR, Dettinger MD (2008) Human-induced changes in the hydrology of the western United States. Science 319: 1080–1083

Blankinship JC, Hart SC (2012) Consequences of manipulated snow cover on soil gaseous emission and N retention in the growing season: a meta-analysis. Ecosphere 3. doi: 10.1890/ES11-00225.1

Boisvenue C, Running SW (2010) Simulations show decreasing carbon stocks and potential for carbon emissions in Rocky Mountain forests over the next century. Ecol Appl 20: 1302–1319

Bond-Lamberty B, Thomson A (2010) Temperature-associated increases in the global soil respiration record. Nature 464:579–582

Borken W, Matzner E (2009) Reappraisal of drying and wetting effects on C and N mineralization and fluxes in soils. Glob Chang Biol 15:808–824

Bowling DR, Grote EE, Belnap J (2011) Rain pulse response of soil CO_2 exchange by biological soil crusts and grasslands of the semiarid Colorado Plateau, United States. J Geophys Res 116:G03028

Brooks PD, McKnight D, Elder K (2005) Carbon limitation of soil respiration under winter snowpacks: potential feedbacks between growing season and winter carbon fluxes. Glob Chang Biol 11:231–238

Camarda M, De Gregorio S, Favara R, Gurrieri S (2007) Evaluation of carbon isotope fractionation of soil CO_2 under an advective-diffusive regimen: a tool for computing the isotopic composition of unfractionated deep source. Geochim Cosmochim Acta 71:3016–3027

Cayan DR, Kammerdiener SA, Dettinger MD, Caprio JM, Peterson DH (2001) Changes in the onset of spring in the western United States. Bull Am Meteorol Soc 82:399–415

Chen S, Lin G, Huang J, Jenerette GD (2009) Dependence of carbon sequestration on the differential responses of ecosystem photosynthesis and respiration to rain pulses in a semiarid steppe. Glob Chang Biol 15:2450–2461

Chou WW, Silver WL, Jackson RD, Thompson AW, Allen-Diaz B (2008) The sensitivity of annual grassland carbon cycling to the quantity and timing of rainfall. Glob Chang Biol 14:1382–1394

Coxson DS, Parkinson D (1987) Winter respiratory activity in aspen woodland forest floor litter and soils. Soil Biol Biochem 19:49–59

Davidson EA, Janssens IA (2006) Temperature sensitivity of soil carbon decomposition and feedbacks to climate change. Nature 440:165–173

de Dato G, De Angelis P, Sirca C, Beier C (2010) Impact of drought and increasing temperatures on soil CO_2 emissions in a Mediterranean shrubland (gariga). Plant Soil 327: 153–166

de Jong E, Schappert HJV (1972) Calculation of soil respiration and activity from CO_2 profiles in the soil. Soil Sci 113: 328–333

DeSutter TM, Sauer TJ, Parkin TB (2006) Porous tubing for use in monitoring soil CO_2 concentrations. Soil Biol Biochem 38:2676–2681

Ehleringer JR, Arnow LA, Arnow T, McNulty IB, Negus NC (1992) Red Butte Canyon research natural area: history, flora, geology, climate, and ecology. Great Basin Nat 52:95–121

Fierer N, Schimel JP (2003) A proposed mechanism for the pulse in carbon dioxide production commonly observed following the rapid rewetting of a dry soil. Soil Sci Soc Am J 67:798–805

Fierer N, Chadwick OA, Trumbore SE (2005) Production of CO_2 in soil profiles of a California annual grassland. Ecosystems 8:412–429

Flechard CR, Neftel A, Jocher M, Ammann C, Leifeld J, Fuhrer J (2007) Temporal changes in soil pore space CO_2 concentration and storage under permanent grassland. Agric For Meteorol 142:66–84

Gamnitzer U, Moyes AB, Bowling DR, Schnyder H (2011) Measuring and modelling the isotopic composition of soil respiration: insights from a grassland tracer experiment. Biogeosciences 8:1333–1350

Gillies RR, Wang S-Y, Booth MR (2012) Observational and synoptic analyses of the winter precipitation regime change over Utah. J Clim 25:4679–4698

Hirsch AI, Trumbore SE, Goulden ML (2002) Direct measurement of the deep soil respiration accompanying seasonal thawing of a boreal forest soil. J Geophys Res 108:8221. doi:10.1029/2001JD000921

Howard DM, Howard PJA (1993) Relationships between CO_2 evolution, moisture content and temperature for a range of soil types. Soil Biol Biochem 25:1537–1546

Journal : Medium 10533 | Dispatch : 21-9-2012 | Pages : 15
Article No. : 9797 | LE | TYPESET
MS Code : BIOG-D-12-00048 | CP | DISK

Hu J, Moore DJP, Burns SP, Monson RK (2010) Longer growing seasons lead to less carbon sequestration by a subalpine forest. Glob Chang Biol 16:771–783. doi: 710.1111/j.1365-2486.2009.01967.x

Hultine KR, Bush SE, West AG, Ehleringer JR (2007) Population structure, physiology and ecohydrological impacts of dioecious riparian tree species of western North America. Oecologia 154:85–93

IPCC (2007) Climate Change 2007: The Physical Science Basis. Contribution of Working Group I to the Fourth Assessment Report of the Intergovernmental Panel on Climate Change. Cambridge University Press, Cambridge

Irvine J, Law BE, Martin JG, Vickers D (2008) Interannual variation in soil CO_2 efflux and the response of root respiration to climate and canopy gas exchange in mature ponderosa pine. Glob Chang Biol 14:2848–2859

Jassal R, Black A, Novak M, Morgenstern K, Nesic Z, Gaumont-Guay D (2005) Relationship between soil CO_2 concentrations and forest-floor CO_2 effluxes. Agric For Meteorol 130:176–192

Kim DG, Vargas R, Bond-Lamberty B, Turetsky MR (2012) Effects of soil rewetting and thawing on soil gas fluxes: a review of current literature and suggestions for future research. Biogeosciences 9:2459–2483

Knowles N, Dettinger MD, Cayan DR (2006) Trends in snowfall versus rainfall in the Western United States. J Clim 19:4545–4559

Kueppers LM, Harte J (2005) Subalpine forest carbon cycling: short- and long-term influence of climate and species. Ecol Appl 15:1984–1999

Liptzin D, Williams MW, Helmig D, Seok B, Filippa G, Chowanski K, Hueber J (2009) Process-level controls on CO_2 fluxes from a seasonally snow-covered subalpine meadow soil, Niwot Ridge, Colorado. Biogeochemistry 95:151–166

Maseyk K, Wingate L, Seibt U, Ghashghaie J, Bathellier C, Almeida P, Lobo de Vale R, Pereira JS, Yakir D, Mencuccini M (2009) Biotic and abiotic factors affecting the $\delta^{13}C$ of soil respired CO_2 in a Mediterranean oak woodland. Isot Environ Health Stud 45:343–359

Massman WJ (1998) A review of the molecular diffusivities of H_2O, CO_2, CH_4, CO, O_3, SO_2, NH_3, N_2O, NO, and NO_2 in air, O_2 and N_2 near STP. Atmos Environ 32: 1111–1127

Miller AE, Schimel JP, Meixner T, Sickman JO, Melack JM (2005) Episodic rewetting enhances carbon and nitrogen release from chaparral soils. Soil Biol Biochem 37: 2195–2204

Millington RJ (1959) Gas diffusion in porous media. Science 130:100–102

Moyes AB, Gaines SJ, Siegwolf RTW, Bowling DR (2010) Diffusive fractionation complicates isotopic partitioning of autotrophic and heterotrophic sources of soil respiration. Plant Cell Environ 33:1804–1819

Munson SM, Benton TJ, Lauenroth WK, Burke IC (2010) Soil carbon flux following pulse precipitation events in the shortgrass steppe. Ecol Res 25:205–211

Olsen HR, Van Miegroet H (2009) Factors affecting carbon dioxide release from forest and rangeland soils in Northern Utah. Soil Sci Soc Am J 74:282–291

Pacific VJ, McGlynn BL, Riveros-Iregui DA, Epstein HE, Welsch DL (2009) Differential soil respiration responses to changing hydrologic regimes. Water Resour Res 45: W07201. doi: 10.1029/2009WR007721

Phillips CL, Nickerson N, Risk D, Bond BJ (2011) Interpreting diel hysteresis between soil respiration and temperature. Glob Chang Biol 17:515–527

Piao SL, Ciais P, Friedlingstein P, Peylin P, Reichstein M, Luyssaert S, Margolis H, Fang JY, Barr A, Chen AP, Grelle A, Hollinger DY, Laurila T, Lindroth A, Richardson AD, Vesala T (2008) Net carbon dioxide losses of northern ecosystems in response to autumn warming. Nature 451: 49–52

Raich JW (1992) The global carbon dioxide flux in soil respiration and its relationship to vegetation and climate. Tellus 44B:81–99

Rayment MB, Jarvis PG (1997) An improved open chamber system for measuring soil CO_2 effluxes in the field. J Geophys Res 102:28779–28784

Richardson AD, Andy Black T, Ciais P, Delbart N, Friedl MA, Gobron N, Hollinger DY, Kutsch WL, Longdoz B, Luyssaert S, Migliavacca M, Montagnani L, William Munger J, Moors E, Piao S, Rebmann C, Reichstein M, Saigusa N, Tomelleri E, Vargas R, Varlagin A (2010) Influence of spring and autumn phenological transitions on forest ecosystem productivity. Philos Trans R Soc B 365:3227–3246

Riveros-Iregui DA, McGlynn BL, Epstein HE, Welsch DL (2008) Interpretation and evaluation of combined measurement techniques for soil CO_2 efflux: discrete surface chambers and continuous soil CO_2 concentration probes. J Geophys Res 113: G04027. doi: 10.1029/2008JG000811

Ryan MG, Law BE (2005) Interpreting, measuring, and modeling soil respiration. Biogeochemistry 73:3–27

Sacks WJ, Schimel DS, Monson RK (2007) Coupling between carbon cycling and climate in a high-elevation, subalpine forest: a model-data fusion analysis. Oecologia 151:54–58

Saetre P, Stark JM (2005) Microbial dynamics and carbon and nitrogen cycling following re-wetting of soils beneath two semi-arid plant species. Oecologia 142:247–260

Schmidt MWI, Torn MS, Abiven S, Dittmar T, Guggenberger G, Janssens IA, Kleber M, Kogel-Knabner I, Lehmann J, Manning DAC, Nannipieri P, Rasse DP, Weiner S, Trumbore SE (2011) Persistence of soil organic matter as an ecosystem property. Nature 478:49–56

Seager R, Ting MF, Held I, Kushnir Y, Lu J, Vecchi G, Huang HP, Harnik N, Leetmaa A, Lau NC, Li CH, Velez J, Naik N (2007) Model projections of an imminent transition to a more arid climate in southwestern North America. Science 316:1181–1184

Simunek J, Saurez DL (1993) Modeling of carbon dioxide transport and production in soil 1. Model development. Water Resour Res 29:487–497

Skopp J, Jawson MD, Doran JW (1990) Steady-state aerobic microbial activity as a function of soil water content. Soil Sci Soc Am J 54:1619–1625

Sperry JS (2000) Hydraulic constraints on plant gas exchange. Agric For Meteorol 104:13–23

Tang JW, Baldocchi DD (2005) Spatial-temporal variation in soil respiration in an oak-grass savanna ecosystem in California and its partitioning into autotrophic and heterotrophic components. Biogeochemistry 73:183–207

Vargas R, Baldocchi DD, Bahn M, Hanson PJ, Hosman KP, Kulmala L, Pumpanen J, Yang B (2011) On the multi-

Journal : Medium 10533 | Dispatch : 21-9-2012 | Pages : 15
Article No. : 9797 | LE | TYPESET
MS Code : BIOG-D-12-00048 | CP | DISK

temporal correlation between photosynthesis and soil CO_2 efflux: reconciling lags and observations. New Phytol. doi: 10.1111/j.1469-8137.2011.03771.x

Wardle DA, Bardgett RD, Klironomos JN, Setälä H, van der Putten WH, Wall DH (2004) Ecological linkages between aboveground and belowground biota. Science 304:1629–1633

Journal : Medium 10533 | Dispatch : 21-9-2012 | Pages : 15
Article No. : 9797 | ☐ LE | ☐ TYPESET
MS Code : BIOG-D-12-00048 | ✔ CP | ✔ DISK